DALTON
FULL PAPER

Crystal structure, solution properties and hydrolytic activity of an alkoxo-bridged dinuclear copper(II) complex, as a ribonuclease model †

Tamás Gajda,*[a] Attila Jancsó,[a] Satu Mikkola,[b] Harri Lönnberg[b] and Holger Sirges[c]

[a] *Department of Inorganic and Analytical Chemistry, University of Szeged, P.O. BOX 440, H-6701 Szeged, Hungary. E-mail: gajda@chem.u-szeged.hu*
[b] *Department of Chemistry, University of Turku, FIN-20500 Turku, Finland*
[c] *Anorganisch-Chemisches Institut der Universität Münster, Wilhelm-Klemm-Straße 8, D-48149 Münster, Germany*

Received 2nd October 2001, Accepted 31st January 2002
First published as an Advance Article on the web 20th March 2002

Crystal structures, solution properties and ribonuclease activity of copper(II) complexes of a binucleating, bis-pyridyl ligand (*N*,*N*′-bis(2-pyridylmethyl)-1,3-diaminopropan-2-ol, **L**) have been investigated. The single-crystal X-ray structure of the mononuclear complex [Cu**L**$(ClO_4)_2$] (**1**) shows distorted octahedral geometry around the metal ion, with the four nitrogens of the ligand in the equatorial plane of copper(II). A μ-alkoxo-bridged dinuclear complex is formed in the presence of a two-fold metal excess. Despite the symmetrical ligand, the two metal ions in $[Cu_2(\mathbf{L}H_{-1})(DPP)(ClO_4)(CH_3OH)]ClO_4$ (**2**, DPP = diphenyl phosphate) have distinct, distorted octahedral (Cu1) and square pyramidal (Cu2) geometry. Beside the alkoxo-oxygen, the phosphate group of DPP also bridges the two metal centers in **2** in a μ-1,3-bridging mode. The complexes formed in aqueous solution are likely to have analogous structures to **1** and **2**. The dinuclear $[Cu_2(\mathbf{L}H_{-1})(OH)]$ complex efficiently promotes the hydrolysis/transesterification of both activated (2-hydroxypropyl *p*-nitrophenyl phosphate, hpnp) and non-activated, biological phosphodiesters (uridine-2′,3′-cyclic-monophosphate, cUMP and uridylyl-(3′,5′)-uridine, UpU). For example, a 2 mM solution of the dinuclear complex provides 5 orders of magnitude acceleration in the hydrolysis of cUMP. The proposed mechanisms include double Lewis-acid activation with intramolecular general base catalysis.

Introduction

Binuclear metallocenters are widely used in metallobiomolecules. In most cases, the two metal ions cooperate with each other, and they frequently share the tasks necessary to accomplish a given function. The design of structural and functional model complexes of such binuclear centers has been the subject of very extensive investigations. Metallophosphoesterases are an important class of those enzymes which frequently operate in binuclear active sites.[1,2] Over the past 10 years great attention has been paid to the development of simple metal complexes able to mimic the function of phosphoester processing enzymes.[3–18] Functional model complexes designed to mimic the binuclear motif of native enzymes, pointed to the great efficiency of bimetallic cooperation during hydrolysis.[10,11] Several effects are recognized by which dinuclear centers may accelerate the cleavage of phosphoester bonds: (i) more efficient substrate binding, (ii) double Lewis-acid activation and (iii) strain in the PO_4 tetrahedron caused by the bridging coordination of substrate.[10] Although several highly active dinuclear complexes have been reported over the years,[12–19] most of these complexes have their own substrate, mechanism or pH selectivity, thus the development of new functional models is of great interest.

Binucleating ligands providing an endogenous μ-1,1 bridging alkoxo unit are widely used to construct bimetallic cores,[20] but only a few zinc(II)[16–18] and nickel(II)[19] complexes of such ligands are reported as efficient functional models for phosphoesterases. Recently, we reported the structure and ribonuclease activity of alkoxo-bridged dinuclear zinc(II) and copper(II) complexes[18] formed with a bis-imidazole ligand (*N*,*N*′-bis(5-methylimidazol-4-ylmethyl)-1,3-diaminopropan-2-ol, bimido). The hydrolytic activity of the copper(II) species was found to be modest compared with the analogous dizinc(II) complex, although the chemical properties of copper(II) would suggest higher activity. In order to retain the favorable properties of this ligand (relatively open coordination sphere for the metal ions, *ca*. 3.5 Å metal–metal separation), but create a hydrolytically more efficient dicopper(II) complex, we synthesized a dinucleating bis-pyridyl ligand (*N*,*N*′-bis(2-pyridylmethyl)-1,3-diaminopropan-2-ol, bpdpo, Scheme 1), related to bimido. Both mono-

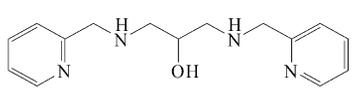

Scheme 1 Schematic structure of bpdpo.

nuclear and dinuclear copper(II) complexes of this ligand have already been prepared,[21,22] but to our knowledge only magnetochemical studies are available for these complexes and their structures are not known. In this paper we report structural and solution chemistry studies of copper(II) complexes of bpdpo, together with kinetic studies on the hydrolysis of both activated and non-activated phosphodiesters, promoted by a dinuclear copper(II) complex.

† Electronic supplementary information (ESI) available: ORTEP representation of a part of the infinite cation chain in **2**. See http://www.rsc.org/suppdata/dt/b1/b108948j/

Experimental

Materials and methods

Copper(II) perchlorate (Fluka) solutions were standardized complexometrically. Potentiometric titrations were performed by Titrisol NaOH standard solution (Merck). MES (2-([*N*-morpholino]ethanesulfonic acid), HEPES, 2′,3′-cUMP (uridine-2′,3′-cyclic-monophosphate, Sigma) and UpU (uridylyl-(3′,5′)-uridine, Sigma) were used without further purification. The barium salt of 2-hydroxypropyl-*p*-nitrophenyl phosphate (hpnp) was prepared according to the literature procedure.[23] UV/VIS spectra were measured on a Hewlett Packard 8452A diode array spectrophotometer. The EPR spectra were recorded on a JEOL-JES-FE 3X spectrometer in the X-band region at 298 K and 77 K with 100 kHz field modulation. Manganese(II)-doped MgO powder was used as field standard. ^{1}H NMR measurements were performed on Bruker Avance DRX 500 spectrometers. The chemical shifts (δ) were measured relative to dioxane as an internal reference and converted relatively to $SiMe_4$, using $\delta_{dioxane} = 3.70$.

Preparation of the ligand *N*,*N*′-bis(2-pyridylmethyl)-1,3-diaminopropan-2-ol·4HCl (L·4HCl)

The compound was prepared by a slight modification of the procedure described previously.[21] To a solution of 1.8 g 1,3-diamino-2-propanol (20 mmol) in 20 mL methanol 4.28 g pyridine-2-carbaldehyde (40 mmol) was added and allowed to react for 12 h at room temperature. The volume of this solution was increased with 30 mL of methanol then 2 g of sodium borohydride was added in small portions while stirring. After 3 h at room temperature, the reaction was completed by refluxing for 1 h. The mixture was evaporated to dryness. The solid was dissolved in 50 mL chloroform and was extracted three times with 10 mL of water. The chloroform layer was dried over anhydrous $MgSO_4$, filtered and evaporated to dryness again. The solid was redissolved in 80 mL absolute ethanol then 8 mL concentrated hydrochloric acid was added. The white precipitate was filtered off and recrystallized twice from methanol. Yield: 5.5 g, 66%. The structure and purity were confirmed by NMR spectroscopy and potentiometry. ^{1}H-NMR (in D_2O, δ): $\delta = 8.77$ (d, $^3J = 5.2$ Hz, 2H, pyrH), 8.42 (m, $^3J = 7.8$ and 8.2 Hz, $^4J = 1.5$ Hz, 2H, pyrH), 7.99 (d, $^3J = 8.2$ Hz, 2H, pyrH), 7.91 (m, $^3J = 7.8$ and 5.2 Hz, 2H, pyrH), 4.45 (m, $^3J = 9.6$ and 3.0 Hz, 1H, C*H*–OH), 3.42 and 3.29 (m, $^2J = 13.0$ Hz, $^3J = 9.6$ and 3.0 Hz, 2H + 2H, CH_2–CH) and 3.29 (s, 4H, pyr–CH_2). No other signal was detected.

Preparation of the complexes

[Cu(L)(ClO$_4$)$_2$] (1). **L**·4HCl (62.1 mg, 0.15 mmol) dissolved in 5 mL of dry methanol was neutralized with 4 equivalents of NaOH (also dissolved in methanol). 55.6 mg (0.15 mmol) $Cu(ClO_4)_2 \cdot 6H_2O$ in 5 mL methanol was then added to the mixture. The resulting deep blue solution was slowly concentrated to *ca*. 4 mL. After slowly cooling the solution to room temperature, deep blue crystals were obtained. Analysis: calc. for $C_{15}H_{20}Cl_2CuN_4O_9$ (534.79): C 33.66, H 3.74, N 10.47; found: C 33.41, H 3.76, N 10.45%.

[Cu$_2$(LH$_{-1}$)(DPP)(CH$_3$OH)(ClO$_4$)]ClO$_4$ (2). DPP = diphenyl phosphate. 82.8 mg **L**·4HCl (0.2 mmol) was dissolved in 6 mL 0.2 M methanolic NaOH solution (6 equivalents) and 50.0 mg diphenylphosphonic acid and 148.4 mg (0.4 mmol) $Cu(ClO_4)_2 \cdot 6H_2O$ in 5 mL methanol were added to this solution. After similar treatment as for **L**·4HCl, deep blue crystals were obtained in 7 days. Analysis: calc. for $C_{28}H_{33}Cl_2Cu_2N_4O_{14}P$ (878.53): C 38.24, H 3.76, N 6.37; found: C 38.26, H 3.78, N 6.40%.

X-Ray crystallography

The unit cell data and diffraction intensities of **1** and **2** were collected on a STOE IPDS diffractometer using Mo-K_α radiation ($\lambda = 0.71073$ Å) at 153(2) K with a sample-to-plate distance of 70 mm. The structures were solved using direct methods[24] and refined[25] by full-matrix least squares methods by minimising the function $\Sigma w(|F_o| - |F_c|)^2$, where F_o and F_c are the observed and calculated structure factors. Anisotropic thermal parameters were used for all non-hydrogen atoms. Hydrogen atoms were included in the refinement using the riding model. The isotropic thermal parameters for the methyl and hydroxyl H atoms were refined with 1.5 times (for all other hydrogen atoms with 1.2 times) U_{eq} of the attached atom. One of the perchlorate anions (Cl(2)O_4^-) in **2** was disordered and modeled with two orientations for O12–O14. The refinement indicated an essentially equal occupancy distribution (0.51(2)/0.49(2)) of the two sites. Further data collection parameters and information related to the structure refinement are collected in Table 1.

CCDC reference numbers 163302 and 163303.

See http://www.rsc.org/suppdata/dt/b1/b108948j/ for crystallographic data in CIF or other electronic format.

Potentiometric measurements

The protonation and co-ordination equilibria were investigated[26] by potentiometric titration in aqueous solution (I = 0.1 M, $NaNO_3$, and T = 298 ± 0.1 K) using an automatic titration set including a Dosimat 665 (Metrohm) autoburette, an Orion 710A precision digital pH-meter and an IBM-compatible PC. An Orion 8103BN semimicro pH glass electrode was calibrated[27] *via* the modified Nernst eqn. (1):

$$E = E_0 + K\log[H^+] + J_H[H^+] + J_{OH}K_w/[H^+] \qquad (1)$$

where J_H and J_{OH} are fitting parameters in acidic and alkaline media for the correction of experimental errors, mainly due to the liquid junction and to the alkaline and acidic errors of the glass electrode; $K_w = 10^{-13.75}$ M^2 is the autoprotolysis constant of water.[28] The parameters were calculated by a non-linear least squares method. Complex formation was characterized by the following general equilibrium process (2):

$$pM + qL + rH \xleftrightarrow{\beta_{M_pL_qH_r}} M_pL_qH_r \qquad (2)$$

$$\beta_{M_pL_qH_r} = \frac{[M_pL_qH_r]}{[M]^p[L]^q[H]^r}$$

where M denotes the metal ion and L the non-protonated (neutral) ligand molecule. The corresponding concentration formation constants ($\beta_{M_pL_qH_r} \equiv \beta_{pqr}$) were calculated using the computer program PSEQUAD.[29] The protonation and complex formation constants were calculated as the average of 4 and 8 independent titrations (50–80 data points per titration), respectively. The metal-to-ligand ratios were varied from 2 : 1 to 1 : 2 with metal-ion concentrations between 5×10^{-4} and 4×10^{-3} mol dm^{-3}.

Kinetic studies

Transesterification of hpnp. The reaction was followed in a buffered aqueous solution (I = 0.1 M ($NaNO_3$), T = 298 K) by detecting the increase in absorption maximum at 400 nm of the *p*-nitrophenolate anion (ε = 18900, pK = 6.98(2)). In all cases 0.02 M buffer (MES or HEPES) was used. The initial concentration of hpnp varied from 0.4 mM to 12 mM. The initial slope method (≤ 4% conversion) was used to determine the pseudo first order rate constants. The reported data are the average of triplicate measurements with a reproducibility better than 10%.

Table 1 Crystal structure data for complexes **1** and **2**

	1	**2**
Chemical formula	$C_{15}H_{20}Cl_2CuN_4O_9$	$C_{28}H_{33}Cl_2Cu_2N_4O_{14}P$
M_r	534.79	878.53
Crystal size/mm	0.24 × 0.32 × 0.48	0.16 × 0.20 × 0.32
Crystal system	Monoclinic	Monoclinic
Space group	$P2_1/c$	$P2_1/c$
a/Å	11.714(2)	7.2856(15)
b/Å	12.817(3)	32.789(7)
c/Å	27.364(6)	15.003(3)
α/°	90	90
β/°	90.77(3)	91.70(3)
γ/°	90	90
V/Å^3	4108.0(14)	3583.7(13)
ρ_{calc}/g cm^{-1}	1.729	1.628
Z	8	4
T/K	153(2)	153(2)
μ/mm^{-1}	1.381	1.451
F(000)	2184	1792
Reflections collected/unique	9079/8674 [R(int) = 0.0383]	27024/6583 [R(int) = 0.0687]
Final R indices (all data)[a]	$R1$ = 0.1496, $wR2$ = 0.1819	$R1$ = 0.0800, $wR2$ = 0.1489
Final R indices [$I > 2\sigma(I)$]	$R1$ = 0.0666, $wR2$ = 0.1534	$R1$ = 0.0599, $wR2$ = 0.1362

[a] $R1$ based on F values, $wR2$ based on F^2.

In a typical experiment, the pH of the solution containing 0.71 mM ligand and 1.42 mM copper(II) was adjusted to the desired value. 2 mL of this solution was equilibrated at 298 K in the spectrophotometer, then 100 μl of 0.02 M hpnp was injected into the solution with efficient mixing. The increase of the absorbance at 400 nm was immediately followed. Second-order rate constants were obtained from plots of first-order rate constants against the concentration of Cu_2LH_{-2} species, calculated from the formation constants (given in Table 4).

Hydrolysis of 2′,3′-cUMP and UpU. Kinetic data were measured by hydrolysing 2′,3′-cUMP or UpU in the presence of copper(II)–bpdpo complexes at 308 K and analysing the unreacted substrate and products (2′,3′-cUMP, uridine-2′-phosphate, uridine-3′-phosphate and small amounts of uridine) by HPLC. The pH of the solutions were measured at 298 K, before initiation of the hydrolysis. The initial substrate concentration was 0.05 mM. 10 aliquots of the reaction solutions were periodically taken up in each run. The progress of the reaction was stopped by mixing 0.1 ml aliquot with equal amount of eluent used for HPLC (0.025 mol dm^{-3} acetate buffer, pH = 4.3, containing 0.1 mol dm^{-3} ammonium chloride). Then the sample was injected into the HPLC column, and was analyzed by Merck and Perkin Elmer HPLC systems. The column was a Merck Lichrospher 100 RP-18 (150 × 4 mm, 5μm) or Hypersil ODS RP-18 (250 × 4.6 mm, 5μm). The UV detection was carried out at 254 nm. The hydrolysis was followed for *ca.* three half-lives by observing the disappearance of the substrate and in all cases displayed pseudo first-order kinetics. The rate constants (k_{obs}) were obtained by using the first order kinetics equation. The reported data are the average of duplicate measurements (reproducibility better than 10%).

Results and discussion

Crystal structures

[CuL(ClO$_4$)$_2$] (1). The asymmetric unit consists of two crystallographically independent, but nearly identical complex molecules (**1a** and **1b**). The molecular structure of **1a** is shown in Fig. 1, selected bond lengths and angles are given in Table 2. Both copper(II) ions have an N_4O_2 coordination environment with the four nitrogens of bpdpo and two oxygens from the perchlorato ligands. The Cu–N distances are between 1.995 and 2.034 Å (average 2.015 Å). The four equatorial nitrogens strongly deviate from their least squares plane (average deviation 0.292 (**1a**) and 0.253 Å (**1b**)), which results in a tetrahedral distortion, with *trans* bond angles N1–Cu1–N3 = 164.2(3)° (165.8(3)°) and N2–Cu1–N4 = 160.2(2)° (162.6(2)°) in **1a** (**1b**). Beside the axially bound O2 perchlorate oxygen (2.498(6) Å for **1a**, 2.527(6) Å for **1b**) one might also consider a weak interaction with the O7 perchlorate oxygen (2.891(7) Å for **1a** and 2.819(6) Å for **1b**), resulting in an octahedral structure strongly distorted towards a square planar/pyramidal geometry. The hydroxyl group is not coordinated to the metal ion, but it is involved, together with the secondary amino groups, in hydrogen bonding interactions with perchlorate oxygens.

Table 2 Selected bond lengths [Å] and angles [°] for **1a** and **1b**

Cu(1)–N(1)	2.010(5)	Cu(1A)–N(1A)	1.998(5)
Cu(1)–N(2)	2.019(5)	Cu(1A)–N(2A)	2.028(6)
Cu(1)–N(3)	2.034(5)	Cu(1A)–N(3)	2.021(6)
Cu(1)–N(4)	1.995(5)	Cu(1A)–N(4)	2.016(5)
Cu(1)–O(2)	2.498(6)	Cu(1A)–O(2)	2.527(6)
Cu(1)–O(7)	2.891(7)	Cu(1A)–O(7)	2.819(6)
N(4)–Cu(1)–N(1)	104.3(2)	N(4A)–Cu(1A)–N(1A)	103.7(2)
N(4)–Cu(1)–N(2)	160.2(2)	N(4A)–Cu(1A)–N(2A)	162.6(2)
N(1)–Cu(1)–N(2)	83.5(2)	N(1A)–Cu(1A)–N(2A)	84.0(2)
N(4)–Cu(1)–N(3)	84.9(2)	N(4A)–Cu(1A)–N(3A)	84.8(2)
N(1)–Cu(1)–N(3)	164.2(3)	N(1A)–Cu(1A)–N(3A)	165.8(3)
N(2)–Cu(1)–N(3)	92.0(2)	N(2A)–Cu(1A)–N(3A)	91.1(2)
O(2)–Cu(1)–O(7)	161.6(2)	O(2A)–Cu(1A)–O(7A)	166.5(2)

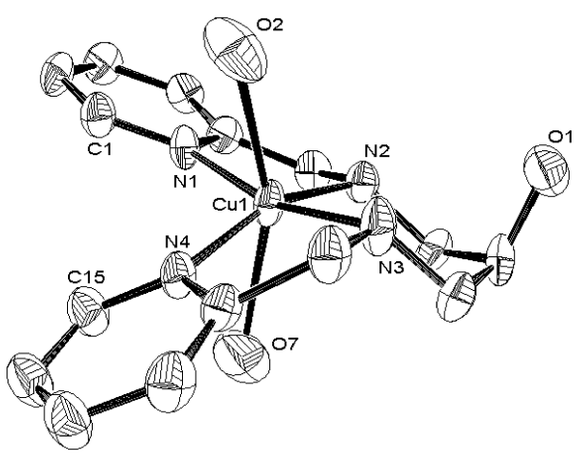

Fig. 1 ORTEP[30] view (50%) of **1** with atom-labelling scheme. Hydrogen atoms and perchlorate ions (except O2 and O7) are omitted for clarity.

Table 3 Selected bond lengths [Å] and angles [°] for **2**

Cu(1)–O(1)	1.914(3)	Cu(2)–O(1)	1.903(3)
Cu(1)–O(2)	1.953(4)	Cu(2)–O(3)	1.938(3)
Cu(1)–N(1)	1.987(4)	Cu(2)–N(4)	1.978(5)
Cu(1)–N(2)	1.989(4)	Cu(2)–N(3)	1.987(4)
Cu(1)–O(8)	2.468(4)	Cu(2)–O(10)	2.332(4)
Cu(1)–O(7a)	2.594(4)	Cu(1) ··· Cu(2)	3.499(1)
O(1)–Cu(1)–O(2)	98.3(2)	O(1)–Cu(2)–O(3)	99.0(2)
O(1)–Cu(1)–N(1)	164.7(2)	O(1)–Cu(2)–N(4)	166.7(2)
O(2)–Cu(1)–N(1)	93.8(2)	O(3)–Cu(2)–N(4)	91.8(2)
O(1)–Cu(1)–N(2)	85.8(2)	O(1)–Cu(2)–N(3)	85.8(2)
O(2)–Cu(1)–N(2)	175.1(2)	O(3)–Cu(2)–N(3)	171.3(2)
N(1)–Cu(1)–N(2)	82.7(2)	N(4)–Cu(2)–N(3)	82.5(2)
O(8)–Cu(1)–O(7a)	170.2(2)	Cu(2)–O(1)–Cu(1)	132.9(2)

Symmetry transformations used to generate equivalent atoms: a $x + 1$, y, z.

$[Cu_2(LH_{-1})(DPP)(CH_3OH)(ClO_4)]ClO_4$ (2). An analogous dinuclear complex of a related bis-imidazole ligand has been recently reported by us.[18] The two complexes possess essentially the same coordination geometry, but differ in fine details. The molecular structure of the dinuclear cation **2** is shown in Fig. 2,

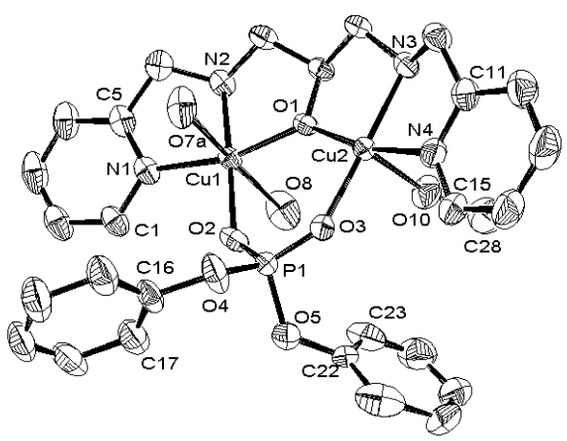

Fig. 2 ORTEP view (30%) of **2** with atom-labelling scheme. Hydrogen atoms and perchlorate ions (except O7a and O8, where O7a is related to O7 by the symmetry operation ($1 + x$, y, z)) are omitted for clarity.

selected bond distances and angles are listed in Table 3. The ligand offers a meridional tridentate chelate coordination for each copper(II) ion, which is bridged by the endogenous μ-alkoxo-oxygen atom and by the exogenous, μ-1,3-bridged phosphate group. Interestingly, the two centers of the dinuclear complex have distinct geometries, in spite of the symmetric nature of bpdpo. Both copper(II) ions are ligated by a pyridyl and a secondary amino nitrogen, and two oxygens from the bridging alkoxo and phosphato group. The coordination sphere of Cu1 is completed by two axially coordinated perchlorate oxygens, forming a distorted octahedral structure with a N_2O_4 donor set. The geometry around Cu2 is distorted square pyramidal with a non-deprotonated methanol oxygen in the apical position (N_2O_3 donor set). In the tetragonal planes of the metal ions the average Cu–N and Cu–O distances are 1.985 and 1.927 Å, respectively. The two axial perchlorate oxygens are 2.468(4) and 2.594(4) Å apart from Cu1, while the bond distance between Cu2 and the methanol oxygen is 2.332(4) Å. All these distances are typical. The equatorial donor atoms of Cu1 strongly deviate from their best plane (average deviation is 0.108 Å), while the basal plane of Cu2 is nearly perfect and the metal ion lies 0.118 Å above this plane. The angle between the two least-squares planes of the metal ions is 16.5(1)° (that of the two pyridyl rings is 28.0(1)°), which results in a tilted structure of the ligand back-bone. The dinuclear units form an infinite cation chain *via* the bridging $Cl(1)O_4^-$ perchlorate groups linking lattice translated Cu1 atoms (see Figure S1 ESI †).

Table 4 Logarithmic formation constants for copper(II) complexes of bpdpo (T = 298 K, I = 0.1 M ($NaNO_3$); $\beta_{pqr} = [M_pL_qH_r]/[M]^p[L]^q[H]^r$, with estimated errors in parentheses (last digit)

pqr	β_{pqr}
011	8.11(1)
012	14.45(1)
013	16.31(3)
014	17.7(2)
110	14.78(1)
21–2	5.33(2)
21–3	−6.06(2)
pK^{21-2}_{21-3}	11.39
NP[a] (FP[b])	605 (0.01 cm^{-3})

[a] NP: number of experimental points. [b] FP: fitting parameter.

The Cu1 ··· Cu2 distance is 3.499(1) Å, the Cu1–O1–Cu2 angle is 132.9(2)°. The bridging coordination mode of DPP results in a considerably distorted tetrahedral geometry around the phosphorus atom. The O2–P1–O3 and O4–P1–O5 angles are 119.6(2)° and 98.2(4)°, respectively; the average P1–O distances for the metal bound oxygens (1.476 Å) are significantly shorter than for O4 and O5 (1.576 Å). These data are similar to those found in other dinuclear complexes containing μ-1,3-bridged phosphate unit(s).[12,18,31] Generally, the "out-of-plane" location of the metal ions, with respect to the phosphinyl-plane, is preferred over the "in-plane" coordination.[32] In the present complex, Cu2 is in, while Cu1 is out of the [P1–O2–O3] plane (the displacement of Cu2 and Cu1 is 0.02(1) and 0.54(1) Å, respectively). For comparison, in the dicopper(II) complex of the related bis-imidazole ligand bimido, the Cu1 and Cu2 ions lie 0.41 and 0.75 Å above the corresponding phosphinyl-plane.[18]

Based on the literature data, the phosphate unit is able to bridge two metal centers when the metal–metal separation is between 3 and 6 Å. In native dinuclear metallo-phosphoesterases the metal–metal distance ranges between 3 and 4 Å,[1,2] and the μ-1,3 bridged phosphoester unit is a frequently occurring substrate binding mode. Complex **2** mimics both of these structural motifs. The Lewis-acid activation, *i.e.* the polarization of the P–O bonds of the substrate, provided by both metal ions (double Lewis-acid activation), is regarded as one of the key features for efficient phosphoester hydrolysis in the case of both dinuclear metallo-phosphoesterases and model complexes. The notable strain in the PO_4 unit, imposed by the μ-1,3 bridging mode, probably facilitates further the nucleophilic attack on the phosphorus atom.[10]

Solution properties

The protonation and complex formation equilibrium have been studied by potentiometry in aqueous solution (I = 0.1 M $NaNO_3$, 298 K), and the results are collected in Table 4. In the case of [Cu(II)] ≤ [bpdpo], the very stable, mononuclear Cu**L** complex is the only species between pH 3 and 11. Two strongly overlapped deprotonations have been observed between pH 6 and 8 in the presence of a two-fold metal excess, leading to the formation of a dinuclear $Cu_2\mathbf{L}H_{-2}$ species (Fig. 3). This complex undergoes a further proton loss around pH 11. Due to the different nature of the pyridyl and imidazole rings, this speciation picture is rather distinct from that observed in the equimolar Cu–bimido system,[18] where CuLH and $CuLH_{-1}$ species were also formed. Solubility problems prevented the speciation study in the Cu(II)/bimido 2 : 1 system, but analogous dinuclear copper(II) and zinc(II) species were detected with some related ligands.[18,33] The high stability and the spectroscopic parameters determined for the complex Cu**L** ($g_\perp$ = 2.061, $g_\parallel$ = 2.221, $A_\parallel$ = 0.0180 T, g_0 = 2.112, A_0 = 0.0074 T, λ^{d-d}_{max} = 602 nm) strongly suggest a 4N coordination in the equatorial plane of copper(II), similar to that found in the crystallographically characterized complex **1**. In the presence of a metal excess, the formation

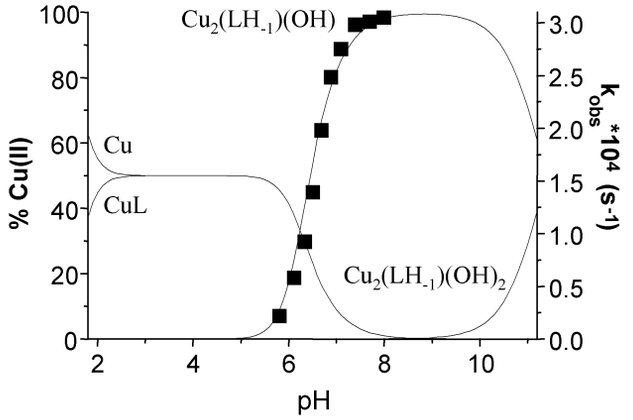

Fig. 3 Species distribution curves (solid lines) and the effect of pH on the transesterification of hpnp (■) in the copper(II)–bpdpo 2 : 1 system (T = 298 K, 2[bpdpo] = [Cu(II)] = 1.4 mM, [hpnp] = 1 mM).

of the dinuclear species causes a gradual decrease of the EPR signal intensity, due to the antiferromagnetically coupled copper(II) centers in $Cu_2\mathbf{L}H_{-2}$. This is also supported by the ^1H NMR spectrum of this species, in which the relatively broad, but easily detectable proton signals are spread over a 100 ppm range (no spectrum could be detected for the mononuclear Cu**L** species). Additionally, the $[Cu\mathbf{L}]^{2+} + Cu^{2+} \rightleftharpoons [Cu_2\mathbf{L}H_{-2}]^{2+} + 2H^+$ process yields some characteristic changes in the electronic spectrum too (see Fig. 4). The isosbestic point around 580 nm

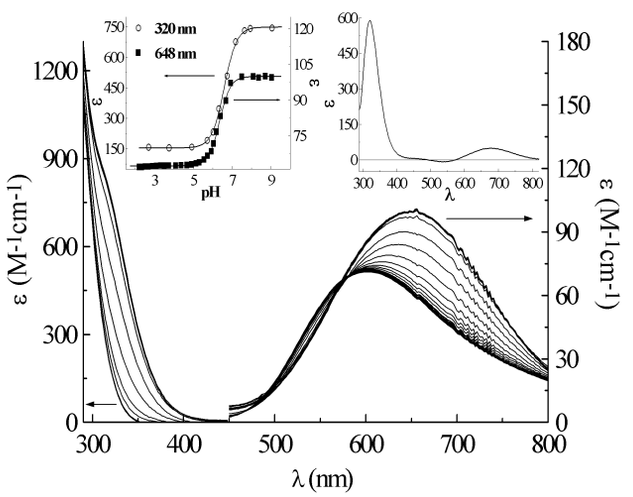

Fig. 4 Effect of pH on the UV/VIS spectra of the copper(II)–bpdpo system in the case of metal excess ([Cu(II)]/[bpdpo] = 2 : 1); the left insert shows the change of absorbance at 320 nm (○) and 648 nm (■), the difference between the spectra of Cu**L** and $Cu_2\mathbf{L}H_{-1}(OH)$ is depicted in the right insert.

indicates a clean transformation from Cu**L** to $Cu_2\mathbf{L}H_{-2}$. The d–d transitions are shifted by 50 nm to higher wavelengths, while only small changes occur in the charge transfer region. Nevertheless, the difference between the spectra of Cu**L** and $Cu_2\mathbf{L}H_{-2}$ shows a distinct band around 324 nm (Fig. 4, insert). Taking into account the ligand structure, the strong antiferromagnetic interaction within the dinuclear complex should imply the endogenous bridging of the alkoxo oxygen. The absorption band observed around 324 nm can be attributed to an LMCT transition of the Cu–O–Cu skeleton.[34] The coordination environment in the equatorial plane of the metal ions changes considerably during this process (from N_4 to N_2O_2), which is in agreement with the observed red shift of the d–d transition. Owing to the lack of any other protonatable group, the second deprotonation in $Cu_2\mathbf{L}H_{-2}$ can be assigned to proton loss from a coordinated water molecule. The resulting hydroxide ion may be bound terminally or form an intramolecular bridge between the metal ions. The large metal–metal separation provided by bpdpo (3.5 Å) prevents μ-1,1 type intramolecular-bridging by the hydroxide ion.[21] Therefore, we propose an analogous single μ-alkoxo bridged structure for the complex $Cu_2\mathbf{L}H_{-2}$ in solution, as determined for complex **2**, with a terminally bound hydroxide ion instead of the bridging DPP moiety. Thus this complex is best described as $[Cu_2(\mathbf{L}H_{-1})(OH)]$. A similar structure was suggested for some related complexes.[18,33]

A notable feature of this system is the low pK of the coordinated water molecule, which is essential in developing efficient phosphoesterase models. The modest hydrolytic activity of a dicopper(II) complex of a related tetra-pyridyl ligand is explained by the crowded coordination sphere of the metal ions.[19] In our case, the tridentate coordination of the ligand does not reduce the Lewis-acidity of the metal ions and allows facile substrate binding to the dimetallic core.

Kinetic studies

Transesterification of hpnp. The equimolar solution of the Cu(II)–bpdpo system does not promote the intramolecular transesterification of hpnp between pH 6 and 11. At two-fold metal excess, however, important transesterification activity developed parallel with the formation of the dinuclear complex $[Cu_2(\mathbf{L}H_{-1})(OH)]$ (Fig. 3), which levels off above pH 7.5, according to the speciation of $[Cu_2(\mathbf{L}H_{-1})(OH)]$. This suggests that the transesterification is promoted by the dinuclear complex, which is further supported by the dependence of the observed rate on the metal-to-ligand ratio (Fig. 5). The rate

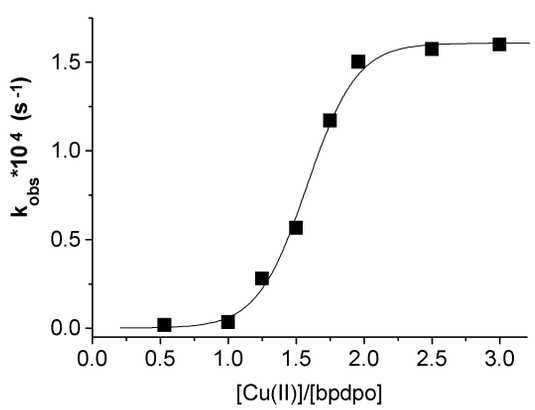

Fig. 5 Dependence of the rate of hpnp transesterification on the [Cu(II)]/[bpdpo] ratio at constant [bpdpo] concentration; pH = 7.5, [bpdpo] = 0.4 mM.

of transesterification increases above 1 : 1 ratio and reaches a plateau at two-fold metal excess, indicating that two metal ions per ligand are required for maximum activity. The rate of hpnp cleavage shows first order dependence on the concentration of the dinuclear species $[Cu_2(\mathbf{L}H_{-1})(OH)]$ (Fig. 6). The second order rate constant, determined from the plot in Fig. 6, is 0.41 M^{-1} s^{-1}. This value is approximatively 5 times higher than that of the hydroxide ion induced transesterification (k_{OH} = 0.0745 M^{-1} s^{-1}).[18]

In order to have better insight into the mechanism, the initial rate of transesterification was measured as the function of substrate concentration. As shown in Fig. 7, above 30-fold excess of substrate, saturation was observed. This indicates a fast pre-equilibrium related to the formation of the catalytically active (catalyst–substrate) complex, followed by the rate determining transformation of the substrate within this complex. The treatment of the data in Fig. 7, using the Michaelis–Menten model, yielded the following constants: k_{cat} = 0.0028 s^{-1} and

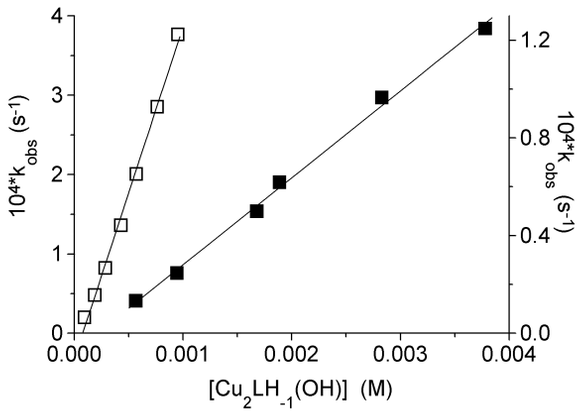

Fig. 6 Dependence of the observed pseudo-first order rate constant on the concentration of [$Cu_2\mathbf{L}_{-1}$(OH)] complex; (□) transesterification of hpnp (T = 298 K, [Cu(II)] = 2[bpdpo], pH = 7.5, [hpnp] = 1 mM), (■) hydrolysis of cUMP (T = 308 K, [Cu(II)] = 2[bpdpo], pH = 7.25, [cUMP] = 50 μM).

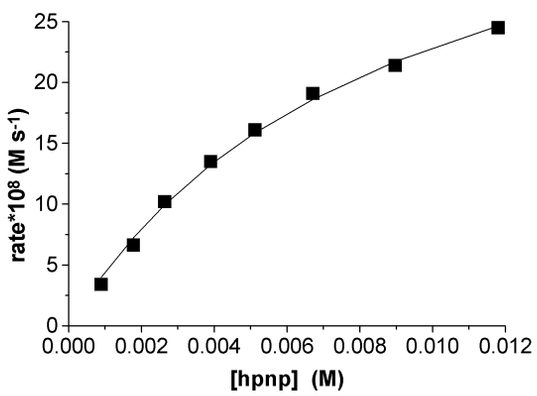

Fig. 7 Saturation kinetic experiments for the transesterification of hpnp (T = 298 K, [Cu(II)] = 2[bpdpo] = 0.3 mM, pH = 7.5).

K_M = 0.0087 M. This catalytic rate constant is slightly greater than the highest value reported to date (0.0026 s^{-1})[14] for di-copper(II) complexes, though k_{cat} values are not available for all highly active systems.[12] Based on these data, the dinuclear complex provides *ca.* 3.5 × 10^4-fold maximal rate acceleration for the transesterification of hpnp at pH 7.5 as compared to the autohydrolysis (k_{auto} = 8.0 × 10^{-8} s^{-1}). The value of the substrate binding constant $K_{ass} \approx 1/K_M$ (115 M^{-1}) value indicates no specific interaction between [Cu_2($\mathbf{L}H_{-1}$)(OH)] and hpnp, and is in the expected range for phosphodiesters.

The [Cu_2($\mathbf{L}H_{-1}$)(OH)] promoted transesterification is catalytic, since four turnovers, obeying first order kinetics, were detected using a four-fold excess of hpnp (2 mM).

Hydrolysis of cUMP and UpU. Ribonucleoside 2′,3′-monophosphates or diribonucleotides provide a direct analogy with the natural substrates of ribonucleases. Therefore, the [Cu_2-$\mathbf{L}H_{-1}$(OH)] mediated hydrolysis/transesterification of both cUMP and UpU were investigated to provide further details on the ribonuclease mimicking activity of the reported system. As can be seen from Fig. 8, the dinuclear complex is able to promote the hydrolysis of both biological substrates. The pH-rate profile for the hydrolysis of cUMP and UpU (Fig. 8) show similar sigmoidal curves as reported for hpnp transesterification. The pK values, determined from the kinetic data at 308 K, are 6.0 and 6.2 for UpU and cUMP, respectively. These data show fairly good agreement with the potentiometric results at identical concentrations (pK 6.25 at 298 K), when the differences in the experimental conditions are also taken into account. The hydrolysis of cUMP shows first order dependence on the concentration of [Cu_2($\mathbf{L}H_{-1}$)(OH)] (Fig. 6). The second order rate constant for the dinuclear complex promoted

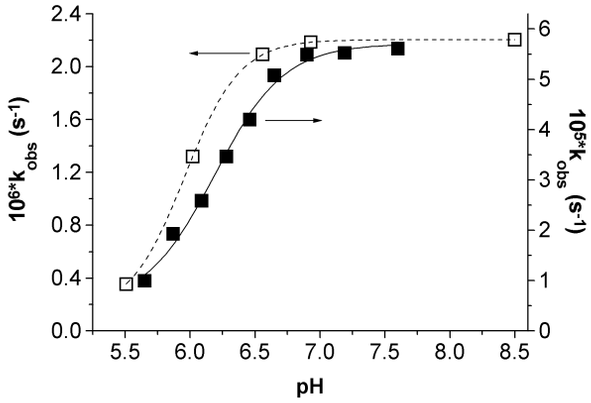

Fig. 8 pH profiles for the hydrolysis of biological phosphates promoted by the copper(II)–bpdpo system (T = 308 K, [Cu(II)] = 2[bpdpo] = 4 mM); (■) hydrolysis of cUMP, (□) hydrolysis of UpU.

hydrolysis of cUMP is 0.036 M^{-1} s^{-1}. This value is about 5 times higher than that of the hydroxide ion promoted hydrolysis (k_{OH} = 0.0065 M^{-1} s^{-1}).[35] Both cUMP and UpU are highly resistant towards hydrolysis. The rate constants for the non-catalyzed hydrolysis at pH 7 and at 308 K, based on the second order rate constants of the hydroxide-catalyzed reactions, are *ca.* 6.5 × 10^{-10} and 4 × 10^{-10} s^{-1} (the corresponding half-lives are 33 and 55 years) for cUMP and UpU,[36] respectively. The presence of 2 mM of the dinuclear complex provides 5 and nearly 4 orders of magnitude rate acceleration (with half-lives of 3 and 87 hours) for cUMP and UpU, respectively. It is also noteworthy, that the dinuclear complex [Cu_2($\mathbf{L}H_{-1}$)(OH)] has 10–20 fold higher hydrolytic efficiency, for the different substrates, compared to its imidazole analogue reported earlier.[18]

Mechanism for phosphodiester hydrolysis. The presented experimental data allow one to draw some mechanistic conclusions. The saturation kinetic experiments indicated that the transesterification of hpnp proceeds through the formation of a catalyst–substrate complex. The X-ray structure data suggest μ-1,3-bridged coordination of the phosphate unit in this active complex, which may provide double Lewis-acid activation for the substrate. The pH-rate profile for the transesterification/hydrolysis reaches a plateau above pH 7–7.5, implying that intramolecular general base catalysis of the metal-bound hydroxide ion should be considered in the case of hpnp and UpU, as shown in Scheme 2. On the other hand, general acid

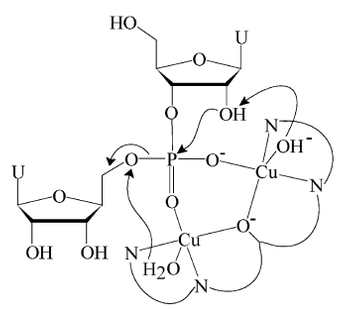

Scheme 2 The proposed mechanism for UpU transesterification.

catalysis by the water molecule coordinated to the second metal ion, may also be considered, since a metal-bound water molecule can assist in the release of the leaving group by protonating the 5′-O^- unit[37] while the catalyst is regenerated by the formation of the M–OH^- residue. Due to the absence of a 2′-OH group, nucleophilic catalysis may also operate in the case of cUMP. The rate acceleration provided by the dinuclear complex is *ca.* 16-fold higher for cUMP than for UpU, as compared with the corresponding autohydrolysis. This relatively low value suggests that general base catalysis is predominant in the case of cUMP hydrolysis, too.

Acknowledgements

T.G. thanks the Alexander von Humboldt Foundation for a research fellowship. This work was supported by the Deutsche Forschungsgemeinschaft, the Hungarian Research Foundation (OTKA T025114 and T037385) and the Foundation of Research Development at Universities (FKFP 0109/2000).

References

1 W. N. Lipscomb and N. Sträter, *Chem. Rev.*, 1996, **96**, 2375.
2 D. E. Wilcox, *Chem. Rev.*, 1996, **96**, 2435.
3 J. N. Morrow, K. Aures and D. Epstein, *J. Chem. Soc., Chem. Commun.*, 1995, 2431.
4 E. Kimura, Y. Kodama, T. Koike and M. Shiro, *J. Am. Chem. Soc.*, 1995, **117**, 8304.
5 N. E. Dixon, R. J. Geue, J. N. Lambert, S. Moghaddas, D. A. Pearce and A. M. Sargeson, *Chem. Commun.*, 1996, 1287.
6 R. Hettich and H. J. Schneider, *J. Am. Chem. Soc.*, 1997, **119**, 5638.
7 I. Zagórowska, S. Kuusela and H. Lönnberg, *Nucleic Acids Res.*, 1998, **26**, 3392.
8 T. Itoh, H. Hisada, Y. Usui and Y. Fujii, *Inorg. Chim. Acta*, 1998, **283**, 51.
9 A. Sreedhara and J. A. Cowan, *J. Biol. Inorg. Chem.*, 2001, **6**, 166.
10 N. H. Williams, B. Takasaki, M. Wall and J. Chin, *Acc. Chem. Res.*, 1999, **32**, 485.
11 R. Krämer and T. Gajda, in *Perspectives on Bioinorganic Chemistry*, ed. R. W. Hay, J. R. Dilwoth and K. Nolan, JAI Press Inc., Stamford, Connecticut, 1999, vol. 4, pp. 207–240.
12 M. Wall, R. C. Hynes and J. Chin, *Angew. Chem., Int. Ed. Engl.*, 1993, **32**, 1633.
13 M. J. Young and J. Chin, *J. Am. Chem. Soc.*, 1995, **117**, 10577.
14 P. Molenveld, J. F. Engbersen and D. N. Reinhoudt, *J. Org. Chem.*, 1999, **64**, 6337.
15 S. Liu and A. D. Hamilton, *Chem. Commun.*, 1999, 587.
16 M. Yashiro, A. Ishikubo and M. Komiyama, *J. Chem. Soc., Chem. Commun.*, 1995, 1793.
17 T. Koike, M. Inoue, E. Kimura and M. Shiro, *J. Am. Chem. Soc.*, 1996, **118**, 3091.
18 T. Gajda, T. R. Krämer and A. Jancsó, *Eur. J. Inorg. Chem.*, 2000, 1635.
19 K. Yamaguchi, F. Akagi, S. Fujinami, M. Suzuki, M. Shionoya and S. Suzuki, *Chem. Commun.*, 2001, 375.
20 T. N. Sorrel, *Tetrahedron*, 1996, **45**; 3 and references therein.
21 W. Mazurek, K. J. Berry, K. S. Murray, M. J. O'Connor, M. R. Snow and A. G. Wedd, *Inorg. Chem.*, 1982, **21**, 3071.
22 W. Mazurek, B. J. Kennedy, K. S. Murray, M. J. O'Connor, J. R. Rodgers, M. R. Snow, A. G. Wedd and P. R. Zwack, *Inorg. Chem.*, 1985, **24**, 3258.
23 D. M. Brown and D. A. Usher, *J. Chem. Soc.*, 1965, 6558.
24 G. M. Scheldrick, SHELXS-86, Program for crystal structure determination, University of Göttingen, Germany, 1986.
25 G. M. Scheldrick, SHELXL-97, Program for crystal structure refinement, University of Göttingen, Germany, 1997.
26 A. Jancsó, T. Gajda, E. Mulliez and L. Korecz, *J. Chem. Soc., Dalton. Trans.*, 2000, 2679.
27 F. J. C. Rosotti and H. Rosotti, *The determination of stability constants*, McGraw-Hill Book Co., New York, 1962, p. 149.
28 E. Högfeldt, in *Stability Constants of Metal-Ion Complexes, Part A. Inorganic Ligands*, Pergamon, New York, 1982, p. 32.
29 L. Zékány and I. Nagypál, in *Computational Methods for the Determination of Formation Constants*, ed. D. J. Leggett, Plenum, New York, 1991.
30 C. K. Johnson, ORTEP, Report ORNL-5138, Oak Ridge National Laboratory, Oak Ridge, TN, 1976.
31 J. W. Yun, T. Tanase and S. Lippard, *Inorg. Chem.*, 1996, **35**, 7590.
32 R. S. Alexander, Z. F. Kanyo, L. E. Chirlian and D. W. Christianson, *J. Am. Chem. Soc.*, 1990, **112**, 933.
33 S. T. Frey, N. N. Murthy, S. T. Weintraub, L. K. Thompson and K. D. Karlin, *Inorg. Chem.*, 1997, **36**, 956.
34 M. Handa, T. Idehara, K. Nakano, K. Kasuga, M. Mikuriya, N. Matsumoto, M. Kodera and S. Kida, *Bull. Chem. Soc. Jpn.*, 1992, **65**, 3241.
35 H. I. Abrash, C. C. S. Cheung and C. Davis, *Biochemistry*, 1967, **6**, 1298.
36 The second order rate constant of the hydroxide ion catalyzed hydrolysis of UpU at pH 7 and at 308 K is *ca.* 4×10^{-3} M^{-1} s^{-1}. P. Järvinen, M. Oivanen and H. Lönnberg, *J. Org. Chem.*, 1991, **56**, 5396.
37 S. Mikkola, E. Stenman, K. Nurmi, E. Yousefi-Salakdeh, R. Strömberg and H. Lönnberg, *J. Chem. Soc., Perkin. Trans. 2*, 1999, 1619.